

# From DC18 to MR07: A Metabolically Stable 4,4'-Oxybisbenzoyl Amide as a Low-Nanomolar Growth Inhibitor of *P. falciparum*

Ivan Bassanini,<sup>\*[a, f]</sup> Silvia Parapini,<sup>[b, f]</sup> Nicoletta Basilico,<sup>[c, f]</sup> Donatella Taramelli,<sup>[d, f]</sup> and Sergio Romeo<sup>[e, f]</sup>

To improve the metabolic stability of a 4,4'-oxybisbenzoyl-based novel and potent (nanomolar-range IC<sub>50</sub>) antiparasmodial agent previously described by us, *in silico*-guided structure-activity relationship (SAR) campaigns have been conducted to substitute its peptide decorations with more metabolically stable residues. The effects of the various structural modifications were then correlated with the antiparasmodial activity *in vitro* in phenotypic assays. Among the several derivatives synthesized and compared with the 3D-pharmacophoric map of

the original lead, a novel compound, characterized by a western *tert*-butyl glycine residue and an eastern 1*S*,2*S*-aminoacyclohexanol, showed low-nanomolar-range antiparasmodial activity, no signs of cross-resistance and, most importantly, 47-fold improved Phase I metabolic stability when incubated with human liver microsomes. These results highlight the efficacy of *in silico*-guided SAR campaigns which will allow us to further optimize the structure of the new lead aiming at testing its efficacy *in vivo* using different routes of administration.

## Introduction

Malaria is a mosquito borne parasitic disease affecting humans and other animals caused by different species of protozoa of the genus *Plasmodium*. In humans the highest case fatality rate is due to *P. falciparum* (*Pf*). The World Health Organization (WHO) reported that in 2020, after almost 20 years of steadily reduction, the malaria deaths increased by the 12% compared

to 2019, up to an estimated 627 000 fatalities, the 77% of them being African children aged under 5 years. Also, in 2020 case incidence in the WHO *African Region*, the most burdened one, increased to 232 per 1000 population compared to 222 per 1000 in 2019, mainly because of disruptions to services during the COVID-19 pandemic.<sup>[1]</sup>

Several attempts to mitigate the effects of the COVID-19 pandemic and reduce malaria incidence and mortality have been envisaged. In October 2021, WHO recommended the RTS,S/AS01 malaria vaccine, called Mosquirix. While this milestone is a remarkable feat, this vaccine is indicated only for the prevention of *Pf* malaria in children living in regions with moderate to high transmission and its effectiveness is approximately 40%. Thus, highly effective vaccines against malaria remain elusive. Artemisinin-based combination treatments (ACTs, *i.e.* the combined use of antimalarial drugs with artemisinin derivatives) are now generally accepted as the best treatments for uncomplicated malaria. As examples, the first-line treatments for *Pf* malaria in the WHO *African Region* include artemether-lumefantrine (AL), artesunate-amodiaquine (AS-AQ), artesunate-pyronaridine (AS-PY) and dihydroartemisinin-piperaquine (DHA-PPQ). However, the spread of drug-resistant *Pf* strains can harm the efficacy of ACTs, and of first line drugs in general as it happened with chloroquine (CQ), enhancing the need of efficacy-monitoring to revise national malaria treatment policies.<sup>[2–9]</sup> Accordingly, antimalarial drug efficacy is monitored through therapeutic efficacy studies (TES), which track clinical and parasitological outcomes among patients receiving antimalarial treatment. Artemisinin partial resistance is specifically monitored using an established list of validated and candidate markers associated with decreased sensitivity to this natural sesquiterpene lactone, like mutations in the *Pfkelch13* gene sequence.<sup>[1]</sup> To prevent a potential public health emergency, there is an urgent need for new antiprotozoal agents<sup>[7,8,10–16]</sup> and

[a] Dr. I. Bassanini

Istituto di Scienze e Tecnologie Chimiche "Giulio Natta"  
Consiglio Nazionale delle Ricerche  
Via Mario Bianco 9, 20131 Milano (Italy)  
E-mail: ivan.bassanini@cnr.it

[b] Prof. S. Parapini

Dipartimento di Scienze Biomediche per la Salute  
Università degli Studi di Milano  
Via Pascal 36, 20133 Milano (Italy)

[c] Prof. N. Basilico

Dipartimento di Scienze Biomediche, Chirurgiche e Odontoiatriche  
Università degli Studi di Milano  
Via Pascal 36, 20133 Milano (Italy)

[d] Prof. D. Taramelli


Dipartimento di Scienze Farmacologiche e Biomolecolari  
Università degli Studi di Milano  
Via Pascal 36, 20133 Milano (Italy)


[e] Prof. S. Romeo

Dipartimento di Scienze Farmaceutiche  
Università degli Studi di Milano  
Via Mangiagalli 25, 20133 Milano (Italy)

[f] Dr. I. Bassanini, Prof. S. Parapini, Prof. N. Basilico, Prof. D. Taramelli,  
Prof. S. Romeo

Centro Interuniversitario di Ricerca sulla Malaria-Italian Malaria Network  
Via Festa del Perdono 7, 20122 Milano (Italy)

 Supporting information for this article is available on the WWW under <https://doi.org/10.1002/cmdc.202200355>

 © 2022 The Authors. ChemMedChem published by Wiley-VCH GmbH. This is an open access article under the terms of the Creative Commons Attribution Non-Commercial NoDerivs License, which permits use and distribution in any medium, provided the original work is properly cited, the use is non-commercial and no modifications or adaptations are made.

specifically of novel antimalarial drugs, with broad therapeutic potential and novel mechanisms of action.

In the recent years, our research group has focused its attention on a novel class of potential antimalarial agents characterized by a pharmacophore never described before as antiplasmodial: a 4,4'-oxybisbenzoyl amide core. As the result of an extended lead optimization process conducted *via* structure activity relationships studies (SAR),<sup>[17–20]</sup> we developed **DC18** (Figure 1A), a peptide-decorated 4,4'-oxybisbenzoyl which demonstrated a nanomolar antiplasmodial activity comparable to the *in vitro* performances of artemisinin.<sup>[21]</sup>

**DC18** resulted active against both chloroquine-sensitive and resistant *Pf* strains ( $IC_{50} = 2.45 \pm 0.85$  nM and  $3.13 \pm 0.60$  nM, respectively) and was found to be remarkably low cytotoxic against healthy human cell line (immortalized human endothelial cell, HMEC-1,  $IC_{50} > 25\,000$  nM) resulting in a promising *in vitro* therapeutic index ( $> 7950$ ).<sup>[21]</sup> Moreover, since **DC18** possesses a chemotype structurally unrelated to any of the known antimalarial drugs, we hypothesized that it could interact with a still-undefined protein target in *Pf*. Thus, **DC18** pharmacophoric core was further investigated *in silico* (Figure 1B) discovering a network of narrow SAR delineating a very specific pattern of stereoselective, polar, lipophilic and H-bonding interactions which supported our initial hypothesis and allowed us to build the molecular fingerprints at the basis of its antiplasmodial activity.<sup>[21]</sup>

In the view of a *in vivo* screening using small mammalian models, **DC18** bioavailability was preliminary assessed in terms of solubility, plasma and hepatic stability as well as by calculating values of predicted microsomal intrinsic clearance ( $Cl_i$ ,  $\mu\text{L} \cdot \text{min}^{-1} \cdot \text{mg}^{-1}$ ).<sup>[22,23]</sup> Interestingly, while possessing a promising “druggability” described by its ligand lipophilic efficiency (LLE = 6.20),<sup>[24–26]</sup> **DC18** *in vitro* metabolic stability was found to be poor: along with a high microsomal intrinsic clearance ( $286 \mu\text{L} \cdot \text{min}^{-1} \cdot \text{mg}^{-1}$  in human microsomes), the

compound showed a low intestinal absorption and a low P-glycoprotein (Pgp) binding.<sup>[21]</sup> In this scenario, the peptide decorations of **DC18** 4,4'-oxybisbenzoyl core (the alkyl side chains of the Ile and Leu amino acid residues) could play a key role in its poor metabolic stability as they represent easily-oxidizable moieties and well-known substrates for the redox/hydrolytic enzymes of Phase I metabolism. Moreover, the presence of 15 rotatable bonds, which endow the molecule with high degrees of conformational freedom, might be the cause of **DC18** poor intestinal absorption.

In this work, we exploited an *in silico*-aided rational approach to optimize the structure of **DC18** aiming at enhancing its bioavailability by substituting the original peptide decorations with metabolically stable, non-proteinogenic amino acids (*i.e.* 2-aminoisobutyric acid (AIB), *tert*-butyl and cyclohexyl glycine) or with (chiral) amino-alcohol moieties. The structural modifications were evaluated both in terms of *in silico* pharmacophore mapping and *in vitro* screening of the antiplasmodial activity of the novel **DC18** analogues obtained. Finally, the *in vitro* metabolic profile of the most promising analogue, **MR07**, a derivative bearing a *tert*-butyl glycine and a 1*S*,2*S*-aminocyclohexanol in place of the native Ile and LeuNH<sub>2</sub>, was evaluated using a murine and a human model.

## Results and Discussion

### Synthetic chemistry

As we previously reported,<sup>[19,21]</sup> non-commercially available *N*-Boc primary amines (i–iv) were prepared by coupling *N*<sup>o</sup>,*N*<sup>o</sup>-dialkyl-alkylen- $\alpha,\omega$ -diamine or a primary aliphatic amine with the corresponding *N*-protected  $\alpha$ -amino acids (Scheme 1); the four enantiomerically enriched (*e.e.*  $> 97\%$ ) 1*R*,2*S*-*cis*, 1*S*,2*R*-*cis*, 1*R*,2*R*-*trans* and 1*S*,2*S*-*trans* stereoisomers of 1,2-aminocyclohexanol were instead commercially available and purchased by Merck®.

As described in our previous reports,<sup>[20,21]</sup> the selected synthetic strategy is a telescopic process made of a series of functional group deprotection and peptide couplings conducted directly on crude reaction media without intermediates purification allowing the fast preparation of libraries of 4,4'-oxybisbenzoyl amides. Accordingly, a small library of fifteen analogues of **DC18** were prepared from commercially available 4,4'-bisbenzoic acid following a straightforward TBTU-based coupling strategy (Scheme 1). Final compounds, isolated as the corresponding HCl salts by means of reversed-phase preparative HPLC and salification with a 1 M HCl aqueous solution, were obtained in a sufficient amount and high degrees of purity to be used in the present study. However, the overall yields of the syntheses, calculated at the end of the whole synthetic process, were generally modest.

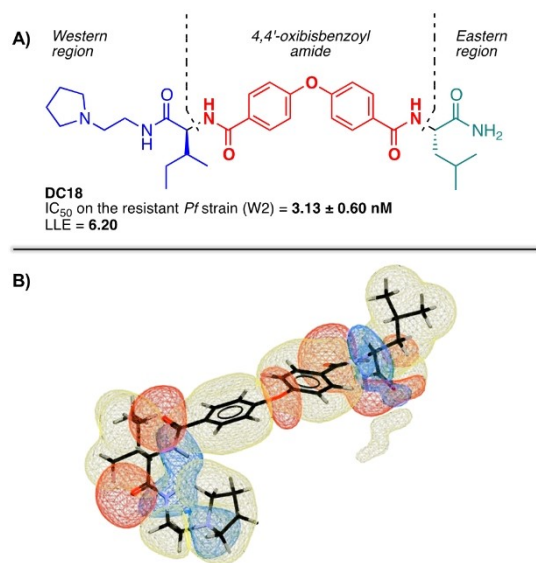
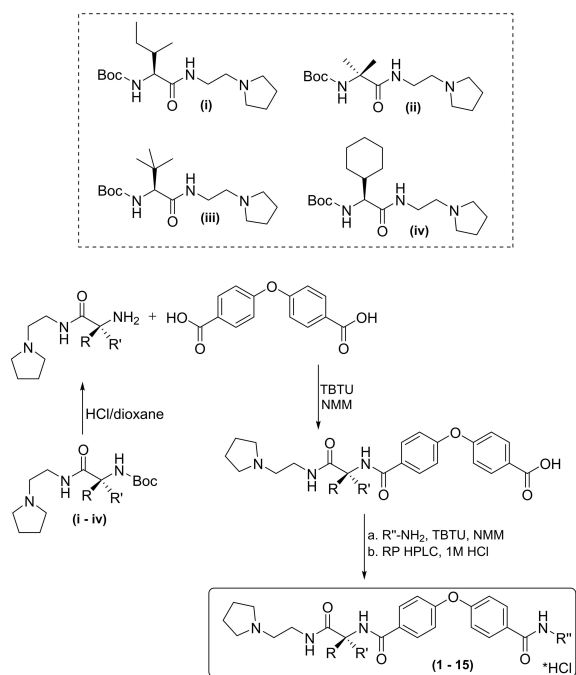


Figure 1. A) Structure and B) force-field pharmacophore mapping of **DC18**.



Scheme 1. Structures of amines i-iv. Synthetic entry to compounds 1-15.

### Antiplasmodial activity

Antiplasmodial activity of compounds 1-15 was tested *in vitro* against the chloroquine-resistant (CQ-R) W2 and the chloroquine-sensitive (CQ-S) D10 strains of *Pf*, using chloroquine (CQ) as reference drug. Results are summarized in Tables 1 and 2.

*In vitro* activity –  $IC_{50}$  (nM) – was expressed as inhibition of parasite growth measuring the activity of parasite lactate dehydrogenase (pLDH).<sup>[27]</sup> Resistance indexes (R.I.), *i.e.* the ratios between the  $IC_{50}$  of each compound against the CQ-R and CQ-S *Pf* strains, were also calculated.

As we previously demonstrated, the *in silico* pharmacophore mapping of DC18 resulted in the definition of very narrow structure activity relationships, specifically in the western region of the molecule in which the pyrrolidine basic head and the sterically-hindered, aliphatic amino acid residue are located and connected by a ethylene linker.<sup>[21]</sup> According to the portion of DC18 that was selected for the insertion of metabolically stable groups and to their nature, the antiplasmodial activities of compounds 1-15 were spread between more than 9  $\mu$ M and less than 2 nM. All compounds that resulted significantly active (2, 5-15;  $IC_{50}^{W2 Pf} < 1 \mu$ M) did not show cross resistance with chloroquine (R.I.s < 1).

### From DC18 to MR07

This work was aimed at improving DC18 metabolic stability *via in silico* driven SAR campaigns. The applied strategy consisted in the rational design of novel synthetic analogues of DC18 containing metabolically stable groups in place of the original

Table 1. Antiplasmodial activity of novel DC18 analogues 1-7.

	R	R <sub>2</sub>	R <sub>3</sub>	D10 $IC_{50}$ [nM]	W2 $IC_{50}$ [nM]	R.I. <sup>[a]</sup>
DC18		H		2.45	3.13	0.31
1	CH <sub>3</sub>	CH <sub>3</sub>		> 9000	> 9000	N.D. <sup>[b]</sup>
2		H		506.3	361.9	0.71
3	CH <sub>3</sub>	CH <sub>3</sub>		> 9000	7529	N.D. <sup>[b]</sup>
4		H		2.89	1.54	0.53
5		H		29.29	17.86	0.60
6		H		74	66	0.89
7		H		60	46	0.76
CQ				20.01	360.12	18

Data are the mean of three experiments run in duplicate; CQ = chloroquine, reference drug. [a] R.I.: resistance index calculated as the ratios between the  $IC_{50}$  of each compound against the CQ-R and CQ-S strains of *P. falciparum*; [b] N.D.: value not defined.

lle and Lue-NH<sub>2</sub> peptide residues *via* the *in silico* prediction of their potential antiplasmodial activity. This was done by exploiting the pharmacophoric fingerprints of DC18 – depicted in Figure 1B as region of donor, acceptor, and non-polar interactions – in a series of ligand overlay experiments.

Briefly, the most energetically favourable conformations of the designed compounds were overlaid with a 3D-pharmacophore map of DC18 obtained from a cluster of highly active 4,4'-oxybisbenzoyl amides ( $IC_{50}^{W2 Pf} < 100$  nM),<sup>[21]</sup> estimating their consistency to the pharmacophoric model. Accordingly, overlay-scores were calculated and normalized to the score of DC18 (see Tables S1 and S2 of Supporting Information): compounds with normalized scores between 0.5 and 1.0 were thus synthesized and tested *in vitro* for their antiplasmodial activity.

Compounds 1-3 (Table 1) were designed to incorporate an AIB residue, a non-stereogenic and conformationally restrained amino acid highly stable toward oxidative metabolism thanks to its *gem*-dimethyl substitution. AIB was used as “probe” to

Table 2. Antiplasmodial activity of compounds 8–15.

	R	R <sub>3</sub>	D10 IC <sub>50</sub> [nM]	W2 IC <sub>50</sub> [nM]	R.I. <sup>[a]</sup>
8 1S, 2R			388	175	0.45
9 1R, 2S			656	359	0.54
10 1R, 2R			391	181	0.46
11 1S, 2S			17.5	7.9	0.45
12 1S, 2R			1042	694	0.66
13 1R, 2S			623	472	0.75
14 1R, 2R			680	587	0.86
15 (MR07) 1S, 2S			24.7	22.8	0.92
CQ			20.01	360.12	18

Data are the mean of three experiments run in duplicate; CQ = chloroquine, reference drug. [a] R.I.: resistance index calculated as the ratios between the IC<sub>50</sub> of each compound against the CQ-R and CQ-S strains of *P. falciparum*.

investigate the effects of the introduction of a conformationally rigid decoration in both the eastern and, most importantly, in the western region of DC18. In agreement with the previously reported SAR, AIB introduction in the western region (compound 3) resulted in a complete loss of antiplasmodial activity ( $IC_{50} > 9 \mu M$ ) with the respect to DC18.

This result highlighted again the importance of stereochemistry, steric hindrance, and backbone flexibility in the western region of this class of antiplasmodials. The same effect was obtained also with compound 1 in which AIB was inserted in both the peptide decoration of DC18 replacing the original Ile and LeuNH<sub>2</sub> residues. Interestingly, when AIB is present only in the eastern region of DC18 (compound 2), a nanomolar antiplasmodial activity against the W2 Pf strain was maintained, even if approximately 100–200-times lower than DC18.

The ligand overlay experiments confirmed this trend: as shown in Figure 2, AIB insertion in the western region produced a conformational restrain in compound 3 (blue) which could not properly fold to arrange into the pharmacophoric pose of DC18 (black). The same was not found for compound 2 (green) which

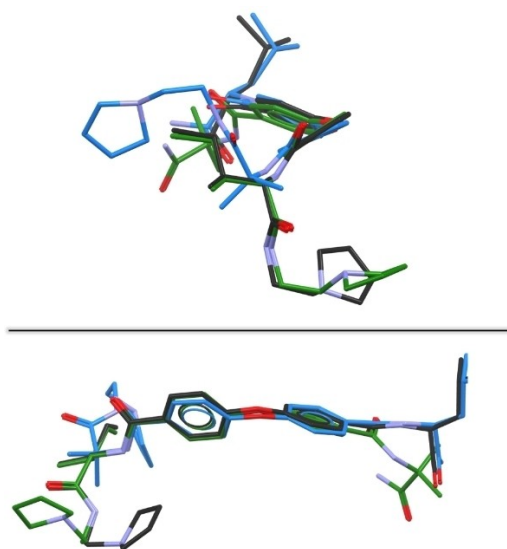


Figure 2. *In silico* overlay of DC18 (black) and compounds 2 (green) and 3 (blue).

anyway presented clear discrepancies between its most energetically favorable pose and DC18 pharmacophore map.

According to the SAR of compounds **1** and **3**, a R-configured, monosubstituted residue connecting the 2-(pyrrolidin-1-yl) ethanamine basic head of the western region with the 4,4'-oxybisbenzoyl core resulted essential for balancing steric hindrance and backbone flexibility in DC18 active conformation. For this reason, compounds **4** and **5** were designed to incorporate in DC18 western region a L-glycine bearing, respectively, a cyclohexyl and *tert*-butyl sidechain as metabolically resistant, monosubstituted residues. Both analogues showed *in silico* a very promising pose in the pharmacophore map resulting in good overlay with DC18 pharmacophoric conformation (Figure 3). Accordingly, *in vitro* screening demonstrated a low nanomolar antiplasmodial activity against the CQ-R W2 *Pf* strain ( $IC_{50} < 20$  nM) for both compounds; the cyclohexyl derivative **4** was found to be even more potent than the parent compound (Figure 3).

Moving the focus to the eastern region of DC18, the analogue **6**, bearing a L-*tert*-butyl glycine in place of the original LeuNH<sub>2</sub> residue, was prepared considering his promising score during *in silico* screening (Table S2, Supporting Information) and the ability of the eastern region of DC18 to accommodate substituents of different steric hindrances and rigidity.<sup>[21]</sup> Compound **6** antiplasmodial activity was found in the nanomolar range. However, this analogue resulted less potent than DC18 (Table 1). Generally speaking an enantiopure R-configured monosubstituted amino acid in DC18 western region seems to be essential for the antiplasmodial activity of this class of compounds.<sup>[21]</sup> Nevertheless, little is known about the possibility of introducing non-peptide decorations in the eastern region. For this reason, our first attempt was the removal of the carboxamide of the eastern region in favour of a primary alcohol as a biologically active moiety able to act as a Lewis-base or a Brønsted-acid. Thus, the leucinol derivative **7**, whose *in silico* score resulted promising (Table S2, Supporting Information), was synthesized and tested: its antiplasmodial activity against both *Pf* strains was found to be in the nanomolar range (Table 1), although the compound was not as potent as DC18.

This first SAR campaign produced a set of *in silico* and *in vitro* data which rationalized the effects of a monosubstitution of the western or of the eastern region in relation to DC18 original antiplasmodial activity. Besides the good

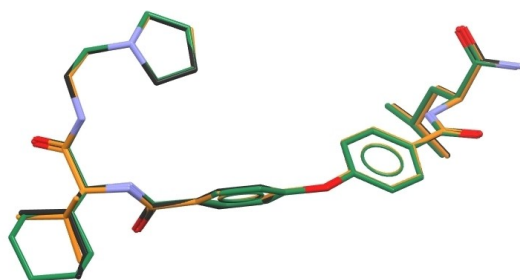


Figure 3. *In silico* overlay of DC18 pharmacophoric conformation (black) and compounds **4** (green) and **5** (orange).

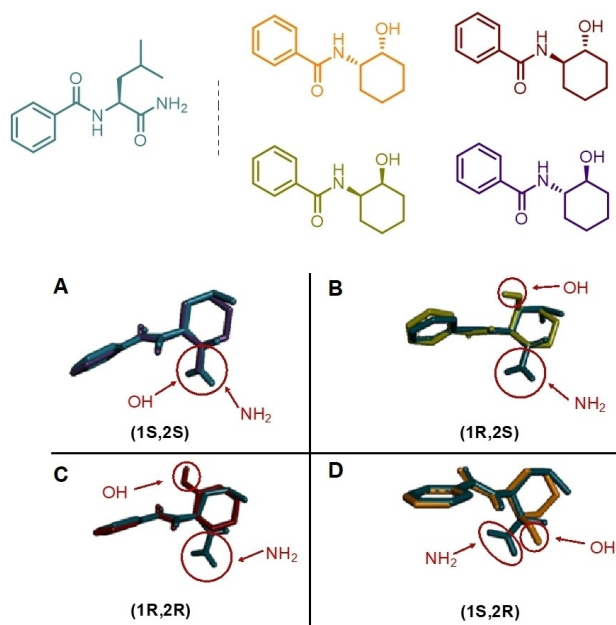
results obtained with the introduction of the metabolically stable *tert*-butyl or cyclohexyl glycine residues in the western region, the substitution of the original LeuNH<sub>2</sub> eastern decoration was of relevance. Accordingly, the discovery that non-amino acid substituents were well tolerated in terms of SAR -provided that the proper stereochemistry, steric hindrance and coordinating groups' orientation were guaranteed- allowed us to design compounds bearing non-peptide eastern decorations.

Thanks to *in silico* screening, 1,2-aminocyclohexanol, a six-membered carbocyclic residue bearing a nitrogenous and an oxygenated coordinating group, was identified as a potential (bio)isostere of the eastern LeuNH<sub>2</sub> residue. Structurally, 1,2-aminocyclohexanol possesses in fact a hindered aliphatic ring able to mimic Leu *iso*-butyl side chain and two coordinating groups in the form of a vicinal amino alcohol moiety that, in the proper stereo-orientation, could establish the same network of interactions built by the original carboxamide residues.

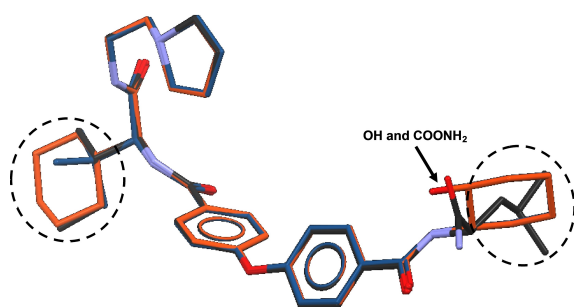
In this scenario, the relative and absolute configuration of the two stereogenic carbons of 1,2-aminocyclohexanol were essential to generate analogues that could properly fit in DC18 pharmacophore. To this purpose, a set of eight novel DC18 derivatives (compounds **8–15**, Table 2) were designed to incorporate the four stereoisomers of 1,2-aminocyclohexanol as eastern decoration (*cis*: 1*S*,2*R* and 1*R*,2*S*; *trans*: 1*S*,2*S* and 1*R*,2*R*) in combination with both L-cyclohexyl or L-*tert*-butyl glycine in the western region as novel analogues formally deriving from compounds **4** and **5**. The scores of all the compounds were found to be higher than the selected threshold of 0.5, with compound **15** possessing the highest one (0.93, Table S2). According to their design, all the compounds of Table 2 were found to be active in the nanomolar range against both the tested *Pf* strains, with no signs of cross-resistance. Among them, the cyclohexyl series (compounds **8–11**) resulted as the most potent. Moreover, the  $IC_{50}$  values of each analogue was strictly dependent on the incorporated 1,2-aminocyclohexanol stereoisomer. Specifically, compounds containing the *trans*-1,2,2*S* isomer (**11** and **15**,  $IC_{50}$  against W2 *Pf* = 7.8 nM and 22.8 nM, respectively) demonstrated the most potent growth inhibitory activity, while the *cis* isomers were generally the worst antiplasmodial agents of the series.

Figure 4 shows a comparison of the *in silico* conformational analysis of a simplified version of DC18 eastern pocket, *i.e.* its *N*-(L-leucine amide) benzamide motif, and of the four stereoisomers of *N*-(2-hydroxycyclohexyl) benzamide, a model of compounds **8–15** eastern decoration. As can be easily seen, the orientation of the –OH and –NH<sub>2</sub> groups of the stereoisomers of *N*-(2-hydroxycyclohexyl) benzamide with the respect to the donor/acceptor *N*-(L-leucine amide)benzamide directly depends on their absolute and relative configurations. According to the *in vitro* results, only the 1*S*,2*S*-*trans*-isomer of *N*-(2-hydroxycyclohexyl)benzamide (Figure 4A) can both assume a conformation in which the –OH and the carboxamide groups are properly overlaid with Leu carboxamide group and arrange the cyclohexane ring to correctly mimic the *iso*-butyl sidechain of the original residue.

Figure 5 shows the *in silico* overlay of the poses of compounds **11** (orange) and **15** (blue) with the active



**Figure 4.** *In silico* overlay of the structural *N*-(*L*-leucine amide)benzamide, i.e. *N*-(1-amino-4-methyl-1-oxopentan-2-yl)benzamide, motif of DC18 (blue) and the four possible (bio)isosteres *N*-((1*S*,2*S*)- (A, purple) *N*-((1*R*,2*S*)- (B, green) *N*-((1*R*,2*R*)- (C, red) and *N*-((1*S*,2*R*)-2-hydroxycyclohexyl)benzamide (D, orange).



**Figure 5.** *In silico* overlay of DC18 active pose (black) with compound 11 (orange) and 15 (blue).

confirmation assumed by DC18 in the pharmacophoric model. The two compounds place their 1,2-aminocyclohexanol ring in the right orientation to mimic the steric features, the backbone flexibility and orientation of the donor/acceptor groups and sterically hindered moiety the LeuNH<sub>2</sub> original residue. Overall, backbone folding and the conformation assumed by the 4,4'-oxybisbenzoyl amide cores, which act as pivot between the eastern and the western regions, are the same in three compounds.

At the end of this SAR campaign, among all the novel DC18 analogues that demonstrated a low-nanomolar antiplasmodial activity, we selected compound 15, named MR07, as the novel lead compound of the series. At variance of compound 11, which showed the highest antiplasmodial activity *in vitro* (Table 2), MR07 is characterized by a western *tert*-butyl glycine residue in place of 11's cyclohexyl glycine decoration. This feature makes MR07 virtually the most stable DC18 analogue

towards both redox and hydrolytic metabolic enzymes. MR07, in fact, is devoid of an easily oxidizable six-membered aliphatic ring and possesses a sterically hindered *tert*-butyl substituent which could, theoretically, protect it from hydrolytic and/or proteolytic enzymatic degradation.

In our previous studies,<sup>[21]</sup> DC18 cytotoxicity was estimated by calculating its *in vitro* selectivity index (IVSI = C<sub>50</sub><sup>HMEC-1</sup>/C<sub>50</sub><sup>W2 PF strain</sup>) against the human cell line HMEC-1. Interestingly, the former lead compound demonstrated both a nanomolar antiplasmodial activity and a remarkably low toxicity *in vitro* with an IVSI > 7950 higher than both chloroquine (IVSI > 58) and dihydroartemisinin (IVSI > 1750) used as reference drugs. MR07 cytotoxicity was thus investigated before moving to its metabolic stability and compared with DC18 performances. Accordingly, MR07 and DC18 were *in vitro* screened against the human cell line Hep G2: both the compounds showed no signs of toxicity up to a concentration of 25 μM, with IVSI > 1096 and > 7987 for MR07 and DC18, respectively.

### MR07: *in vitro* metabolism

The intrinsic clearance (*Cl*<sub>i</sub>) is a parameter that can be easily calculated from *in vitro* experiments that allows to estimate the "phase I" metabolic stability of a drug candidate.<sup>[22,23]</sup> Specifically, a compound is incubated in different conditions in the presence of mammalian (murine or human) liver microsomes in a set of experiments in which its *Cl*<sub>i</sub> is compared with known metabolically stable and easily metabolized compound, like propranolol and 7-ethoxycoumarin (7-EC), respectively. Compounds with *Cl*<sub>i</sub> values higher than 48 μL·min<sup>-1</sup>·mg<sup>-1</sup> are regarded as highly metabolized while *Cl*<sub>i</sub>s lower than 1.8 μL·min<sup>-1</sup>·mg<sup>-1</sup> generally characterize metabolically stable drug candidates (Table 3).<sup>[28–30]</sup>

MR07 intrinsic clearance (*Cl*<sub>i</sub>) was measured *in vitro* in the presence of both murine (see Table S3 of Supporting Information) and human liver microsomes (Table 3) and compared to previously reported data for DC18 and with the *Cl*<sub>i</sub> of propranolol and 7-EC. The phase I metabolic stability of MR07 was found to be remarkably high with a *Cl*<sub>i</sub> value 6.0 ± 0.2 μL·min<sup>-1</sup>·mg<sup>-1</sup>, lower than the reference compound propranolol (24.0 ± 3.8 μL·min<sup>-1</sup>·mg<sup>-1</sup>). As we reported previously,<sup>[21]</sup>

Table 3. Phase I stability in human liver microsomes.			
Compound	<i>Cl</i> <sub>i</sub> <sup>[a]</sup> [μL·min <sup>-1</sup> ·mg <sup>-1</sup> ]	t <sub>1/2</sub> <sup>[b]</sup> [min]	Remaining Percentage [%] <sup>[c]</sup>
MR07	6.0 ± 0.2	232.3 ± 7.5	84 ± 2.8
DC18	286 ± 22 <sup>[d]</sup>	N.D. <sup>[e]</sup>	9 ± 2 <sup>[d]</sup>
7-EC	145.8 ± 44.3	10.0 ± 3.0	17.2 ± 1.0
Propranolol	24.0 ± 3.8	58.6 ± 9.3	54 ± 3.3

[a] Intrinsic Clearance (*Cl*<sub>i</sub>) = k/microsomal concentration × 1000; where k (min<sup>-1</sup>) was derived from the exponential decay equation (peak area/IS vs time) and the microsomal protein concentration used was equal to 0.5 mg protein mL<sup>-1</sup>; [b] Half-life (t<sub>1/2</sub>) = time required for a compound to reduce its concentration to the half of its initial value; [c] Calculated after 60 minutes of incubation; [d] Previously reported data<sup>[21]</sup>; [e] N.D.: value not defined.

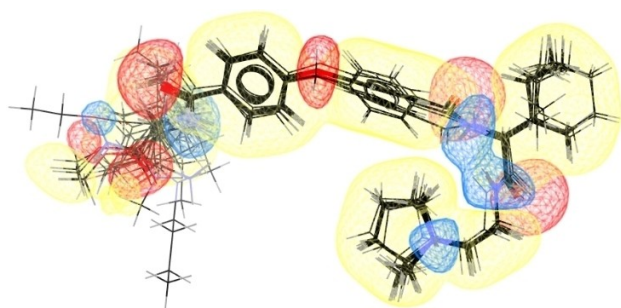


**Figure 6.** Force-field representation of the up-dated pharmacophore model for **MR07**: the areas of donor, acceptor and non-polar interaction are highlighted in red, blue, and yellow, respectively.

**DC18** demonstrated a pretty low metabolic stability with a *Cl* value of  $286 \pm 22 \mu\text{L min}^{-1} \cdot \text{mg}^{-1}$  higher than the *Cl* of the fast-metabolized **7-EC**. When compared to **DC18**, the *Cl* of **MR07** was improved by a 47-fold factor. Accordingly, 84% of **MR07** was recovered after 60 minutes of incubation while only the 9% of **DC18** remained intact in the same assay conditions. *Cl* data for **MR07** and **DC18** in the presence of murine microsomes are reported in **Table S4** (Supporting Information). Moreover, the calculated half-life ( $t_{1/2}$ ) of **MR07** was found to be higher than 200 minutes, further highlighting how the *ad hoc* installed structural modifications significantly improved its metabolic profile *in vitro* and, theoretically, its bioavailability.

## Conclusion

In this work, which is a direct follow-up the detailed SAR investigation campaigns that lead us to the discovery of the potent antiplasmodial **DC18**,<sup>[21]</sup> novel 4,4'-oxybisbenzoyl based potential antimalarial drugs have been rationally designed, prepared and screened *in vitro* aiming at improving the poor metabolic stability of the parent compound. In our quest, *in silico* guided SAR campaigns have been conducted to substitute **DC18** peptide decorations with metabolically stable residues that could properly fit into its 3D-pharmacophoric map which was used as a template to evaluate the effects of the different structural modifications on the antiplasmodial activity.

**MR07**, characterized by a western *tert*-butyl glycine residue and an eastern 1*S*,2*S*-aminocyclohexanol ring in place of the original Ile and LeuNH<sub>2</sub> residues, showed a nanomolar antiplasmodial activity, no signs of cross-resistance and, most importantly, a 47-fold improved phase I metabolic stability compared to **DC18** when incubated with human liver microsomes.

Moreover, thanks to this work, novel portions of the chemical space available in the decoration of the 4,4'-oxybisbenzoic acid core of this class of compounds have been investigated expanding the *in silico* information available around this innovative antiplasmodial pharmacophore. A new map of its features has been thus obtained (Figure 6) and will be used to further optimize **MR07** aiming at testing its efficacy

*in vivo* using different routes of administration or *ad hoc* designed systems for drug delivery.<sup>[31,32]</sup> Also, classical and innovative methods of proteomics analysis<sup>[33–35]</sup> will be used to identify and characterize the nature of the protein target(s) of this class of potent and selective antiplasmodials whose mechanism of action is still unknown.

## Experimental Section

### Synthetic chemistry

#### Materials and methods

All commercially available reagents and solvents were used without further purification.

NMR spectra were recorded on a Varian Mercury 300 VX spectrometer in CD<sub>3</sub>OD, CDCl<sub>3</sub> or DMSO-*d*<sub>6</sub>; chemical shifts were reported in ppm ( $\delta$ ). Peaks were assigned with 2D COSY experiments and agree with the proposed structures.

TLC analyses were carried out on Merck precoated 60 F254 plates using UV light and dipping with or a 10% w/v ethanolic solution of ninhydrin.

Organic phases were dried over anhydrous sodium sulphate. Concentrations were performed under diminished pressure (1–2 kPa) at a bath temperature of 40 °C.

Flash column chromatography was performed using silica gel 60 (0.040–0.063 mm, Merck).

ESI-HRMS were recorded on an ICR-FTMS APEX II (Bruker Daltonics) mass spectrometer.

Preparative HPLC purifications were performed using CH<sub>3</sub>CN/H<sub>2</sub>O + CF<sub>3</sub>COOH gradient and a Waters 2525 Binary Gradient Module equipped with an Agilent Zorbax SB-C18 column.

Purities of final compounds were determined by HPLC using CH<sub>3</sub>CN/H<sub>2</sub>O + CF<sub>3</sub>COOH gradient and a Purospher RP18 5  $\mu\text{m}$  column on a Hitachi Elite Lachrom Instrument equipped with a DAD detector.

#### General procedure A: synthesis of non-commercially available amines

TBTU was added (1.1 eq) to a cooled DCM solution (5 mL mmol<sub>amine</sub><sup>-1</sup>) of the selected primary amine (1.0 eq) and the desired *Boc*-protected  $\alpha$ -amino acid. Subsequently, pH was set at 8 using NMM and the reaction was stirred at room temperature overnight. The mixture was then washed three times with a saturated aqueous solution of NaHCO<sub>3</sub>, two times with water and brine and finally dried over Na<sub>2</sub>SO<sub>4</sub> and concentrated *in vacuo*. The crude product was purified by flash column chromatography on silica gel using a gradient of MeOH in DCM as mobile phase affording the desired *N*-protected amines (i–iv). The desired *N*-*Boc* amine was dissolved in a dioxane solution of HCl (2 M) and stirred at room temperature for 3 hours. After that, solvent was removed *in vacuo* affording the corresponding primary amine which was used without any further purification.

## General procedure B: synthesis of compounds 1–15

TBTU (1.25 g, 3.87 mmol, 1.1 eq) were added to a DMF solution (250 mL) of 4,4'-oxybisbenzoic acid (1 g, 3.87 mmol, 1.1 eq) and of a selected amine (47.0 mmol, 1.0 eq) which was cooled at 0 °C. After setting the pH at 8 by adding NMM, the reaction mixture was stirred at room temperature overnight. DMF was then removed *in vacuo* and the residue was taken up in AcOEt (250 mL). After washing with water (150 mL, 2×), brine (150 mL), the combined organic layers were dried and concentrated *in vacuo*.

The obtained residue was dissolved again in 250 mL of dry DMF and subjected to a second coupling reaction with a different primary amine following the procedure described above which was followed by the same work up procedure affording a crude mixture of coupled products.

Finally, target compounds 1–15 were isolated and purified by RP preparative HPLC and converted into the corresponding hydrochloride salts using a 1 M aqueous solution of hydrochloric acid. Isolated yields were calculated with the respect of the amount of acid reacted in the first coupling.

## Biology

### *Pf* cultures and drug susceptibility assay

*Plasmodium falciparum* cultures were carried out according to Trager and Jensen with slight modifications.<sup>[36]</sup> The CQ-susceptible strain D10 and the CQ-resistant strain W2 were maintained at 5% hematocrit (human type A-positive red blood cells) in RPMI 1640 (EuroClone, Celbio) medium with the addition of 1% AlbuMax (Invitrogen, Milan, Italy), 0.01% hypoxanthine, 20 mM HEPES, and 2 mM glutamine. All the cultures were maintained at 37 °C in a standard gas mixture consisting of 1% O<sub>2</sub>, 5% CO<sub>2</sub>, and 94% N<sub>2</sub>. Compounds were dissolved in DMSO and then diluted with medium to achieve the required concentrations (final DMSO concentration < 1%, which is non-toxic to the parasite). Drugs were placed in 96-well flat-bottomed microplates and serial dilutions made. Asynchronous cultures with parasitaemia of 1–1.5% and 1% final hematocrit were aliquoted into the plates and incubated for 72 h at 37 °C. Parasite growth was determined spectrophotometrically (OD<sub>650</sub>) by measuring the activity of the parasite lactate dehydrogenase (pLDH), according to a modified version of the method of Makler in control and drug-treated cultures.<sup>[27]</sup> The antimalarial activity is expressed as 50% inhibitory concentrations (IC<sub>50</sub>); each IC<sub>50</sub> value is the mean of three experiments run in duplicates.

### Metabolic stability

Test compounds in duplicate were dissolved in DMSO to obtain 0.2 mM solutions and pre-incubated, at the final concentration of 1 μM, for 10 min at 37 °C in potassium phosphate buffer 50 mM pH 7.4, 3 mM MgCl<sub>2</sub>, with mouse and human liver microsomes (Xenotech) at the final concentration of 0.5 mg/mL.

After the pre-incubation period, the reaction was started by adding the cofactors mixture (NADP, Glc6P, Glc6P-DH in 2% sodium bicarbonate); samples (25 μL) were taken at time 0, 10, 20, 30 and 60 min added to 150 μL of a 0.02 μM acetonitrile solution of Verapamil used as Internal Standard (IS) to stop the reaction. After centrifugation the supernatants were analyzed by LC-MS/MS. A control sample without cofactors was added to check the stability of test compounds in the matrix after 60 min. 7-ethoxycoumarin (7-EC) and propranolol were added as reference standards. Sample and data analysis are reported in Supporting Information.

## Cytotoxicity against Hep G2 cell line

Hep G2 is a cell line exhibiting epithelial-like morphology that was isolated from a hepatocellular carcinoma. Cells were maintained in standard conditions at 37 °C in 5% CO<sub>2</sub> incubator in DMEM medium, supplemented with 10% fetal calf serum, 2 mM glutamine, 100 U/mL penicillin, 100 mg/mL Streptomycin. For the toxicity experiments, Hep G2 cells at 1.5 × 10<sup>4</sup> cells/100 μL per well were plated in 96-well plates and incubated at 37 °C, 5% CO<sub>2</sub> overnight. Cells were then treated with serial dilutions of test compounds for 72 h, and cell proliferation was evaluated by using the MTT assay already described.<sup>[37]</sup>

## In silico experiments

### Ligand overlay and expansion of the pharmacophore model

The CCDC-suite (<https://www.ccdc.cam.ac.uk/>) was used for the conformational-based ligand overlay and pharmacophore mapping experiments. Briefly, the structures of the active analogues synthesized in this work (4–7, 11 and MR07 (15); IC<sub>50</sub><sup>W2-Pf strain</sup> < 100 nM) were refined by assigning atomic types, adding a formal positive charge on the basic groups with the DiscoveryStudio and cleaned-up with a Dredging-like force field; then the Mercury module of the CCDC-suite was used to generate 200 conformers for each analogue. Using the Hermes module, a pharmacophore refinement was performed working with the mentioned clusters of conformers and the previously reported pharmacophore model (see Supporting Information).<sup>[21]</sup> The obtained overlays were screened on the base of their internal energy and statistical relevance and the most promising (refined) pharmacophore model was then visualized both as a 'vector and dot' and a surface-field representation and used to extract the structures overlay reported in Figures 2, 3 and 5.

## Acknowledgements

This work was supported by Ministero dell'Istruzione, dell'Università e della Ricerca [PRIN 2015.4JRJPP\_004] and University of Milan "Piano sostegno alla Ricerca, Linea 2 2018" "to SR, Piano sostegno alla Ricerca, Linea 2 2020–2021 to NB and SP. We also thank the Immunohaematology and Transfusion Medicine Service, Department of Laboratory Medicine, ASST Grande Ospedale Metropolitano Niguarda (Milano) for providing erythrocytes for parasite cultures. We also thank Dr. Ugo Zanelli for pharmacokinetic studies. Open Access funding provided by Consiglio Nazionale delle Ricerche within the CRUI-CARE Agreement.

## Conflict of Interest

The authors declare no conflict of interest.

## Data Availability Statement

The data that support the findings of this study are available in the supplementary material of this article.



**Keywords:** *Plasmodium falciparum* · Antimalarials · Malaria · *In silico* pharmacophore mapping · *In vitro* metabolic stability

- [1] World Health Organization, *World Malaria Report 2021*.
- [2] E. Y. Klein, *Int. J. Antimicrob. Agents* **2013**, *41*, 311–317.
- [3] R. T. Gazzinelli, P. Kalantari, K. A. Fitzgerald, D. T. Golenbock, *Nat. Rev. Immunol.* **2014**, *14*, 744–757.
- [4] A. M. Dondorp, P. Ringwald, *Trends Parasitol.* **2013**, *29*, 359–360.
- [5] O. Miotto, J. Almagro-Garcia, M. Manske, B. MacInnis, S. Campino, K. A. Rockett, C. Amarantunga, P. Lim, S. Suon, S. Sreng, J. M. Anderson, S. Duong, C. Nguon, C. M. Chuor, D. Saunders, Y. Se, C. Lon, M. M. Fukuda, L. Amenga-Etego, A. V. O. Hodgson, V. Asoala, M. Imwong, S. Takala-Harrison, F. Nosten, X. Z. Su, P. Ringwald, F. Ariey, C. Dolecek, T. T. Hien, M. F. Boni, C. Q. Thai, A. Amambua-Ngwa, D. J. Conway, A. A. Djimdé, O. K. Doumbo, I. Zongo, J. B. Ouedraogo, D. Alcock, E. Drury, S. Auburn, O. Koch, M. Sanders, C. Hubbard, G. Maslen, V. Ruano-Rubio, D. Jyothi, A. Miles, J. O'Brien, C. Gamble, S. O. Oyola, J. C. Rayner, C. I. Newbold, M. Berriman, C. C. A. Spencer, G. McVean, N. P. Day, N. J. White, D. Bethell, A. M. Dondorp, C. V. Plowe, R. M. Fairhurst, D. P. Kwiatkowski, *Nat. Genet.* **2013**, *45*, 648–655.
- [6] L. Cui, S. Mharakurwa, D. Ndiaye, P. K. Rathod, P. J. Rosenthal, *Am. J. Trop. Med. Hyg.* **2015**, *93*, 57–68.
- [7] M. A. Shibeshi, Z. D. Kifle, S. A. Atnafie, *Infect. Drug Resist.* **2020**, *13*, 4047–4060.
- [8] T. M. Belete, *Drug Des. Dev. Ther.* **2020**, *14*, 3875–3889.
- [9] W. Amelo, E. Makonnen, *BioMed Res. Int.* **2021**, *2021*, DOI 10.1155/2021/5539544.
- [10] I. Bassanini, S. Parapini, N. Basilico, A. Sparatore, *ChemMedChem* **2019**, *14*, 1940–1949.
- [11] I. Bassanini, S. Parapini, E. E. Ferrandi, E. Gabriele, N. Basilico, D. Taramelli, A. Sparatore, *Biomol. Eng.* **2021**, *11*, 56.
- [12] M. Ortalli, S. Varani, G. Cimato, R. Veronesi, A. Quintavalla, M. Lombardo, M. Monari, C. Trombini, *J. Med. Chem.* **2020**, *63*, 13140–13158.
- [13] E. O. J. Porta, I. B. Verdagner, C. Perez, C. Banchio, M. F. de Azevedo, A. M. Katzin, G. R. Labadie, *MedChemComm* **2019**, *10*, 1599–1605.
- [14] S.-M. Lee, M.-S. Kim, F. Hayat, D. Shin, *Molecules* **2019**, *24*, 3886.
- [15] M. A. Shibeshi, Z. D. Kifle, S. A. Atnafie, *Infect. Drug Resist.* **2020**, *13*, 4047–4060.
- [16] S. Kumar, T. R. Bhardwaj, D. N. Prasad, R. K. Singh, *Biomed. Pharmacother.* **2018**, *104*, 8–27.
- [17] S. Romeo, B. M. Dunn, D. Taramelli, E. Bosisio, N. Vaiana, P. Liu, M. Dell'Agli, A. Sparatore, G. Galli, S. Parapini, *J. Med. Chem.* **2006**, *49*, 7440–7449.
- [18] S. Romeo, S. Parapini, M. Dell'Agli, N. Vaiana, P. Magrone, G. Galli, A. Sparatore, D. Taramelli, E. Bosisio, *ChemMedChem* **2008**, *3*, 418–420.
- [19] N. Vaiana, M. Marzahn, S. Parapini, P. Liu, M. Dell'Agli, A. Pancotti, E. Sangiovanni, N. Basilico, E. Bosisio, B. M. Dunn, D. Taramelli, S. Romeo, *Bioorg. Med. Chem. Lett.* **2012**, *22*, 5915–5918.
- [20] A. Pancotti, S. Parapini, M. Dell'Agli, L. Gambini, C. Galli, E. Sangiovanni, N. Basilico, E. Bosisio, D. Taramelli, S. Romeo, *MedChemComm* **2015**, *6*, 1173–1177.
- [21] I. Bassanini, S. Parapini, C. Galli, N. Vaiana, A. Pancotti, N. Basilico, D. Taramelli, S. Romeo, *ChemMedChem* **2019**, *14*, 1982–1994.
- [22] A. Nencini, C. Castaldo, T. A. Comery, J. Dunlop, E. Genesis, C. Ghiron, S. Haydar, L. Maccari, I. Micco, E. Turlizzi, R. Zanaletti, J. Zhang, *Eur. J. Med. Chem.* **2014**, *78*, 401–418.
- [23] C. Ghiron, S. N. Haydar, S. Aschmies, H. Bothmann, C. Castaldo, G. Cocconcelli, T. A. Comery, L. Di, J. Dunlop, T. Lock, A. Kramer, D. Kowal, F. Jow, S. Grauer, B. Harrison, S. La Rosa, L. MacCari, K. L. Marquis, I. Micco, A. Nencini, J. Quinn, A. J. Robichaud, R. Roncarati, C. Scali, G. C. Terstappen, E. Turlizzi, M. Valacchi, M. Varrone, R. Zanaletti, U. Zanelli, *J. Med. Chem.* **2010**, *53*, 4379–4389.
- [24] I. D. K. Untz, K. C. Hen, K. A. S. Harp, P. A. K. Ollman, *Proc. Natl. Acad. Sci. USA* **1999**, *96*, 9997–10002.
- [25] A. L. Hopkins, C. R. Groom, A. Alex, *Drug Discovery Today* **2004**, *9*, 430–431.
- [26] A. L. Hopkins, G. M. Keserü, P. D. Leeson, D. C. Rees, C. H. Reynolds, *Nat. Rev. Drug Discovery* **2014**, *13*, 105–121.
- [27] M. T. Makler, J. M. Ries, J. A. Williams, J. E. Bancroft, R. C. Piper, B. L. Gibbins, D. J. Hinrichs, *Am. J. Trop. Med. Hyg.* **1993**, *48*, 739–741.
- [28] B. Davies, T. Morris, *Pharm. Res.* **1993**, *10*, 1093–5.
- [29] J. Brian Houston, *Biochem. Pharmacol.* **1994**, *47*, 1469–1479.
- [30] R. J. Riley, D. F. McGinnity, R. P. Austin, *Drug Metab. Dispos.* **2005**, *33*, 1304–1311.
- [31] G. Fumagalli, L. Polito, E. Colombo, F. Foschi, M. S. Christodoulou, F. Galeotti, D. Perdicchia, I. Bassanini, S. Riva, P. Seneci, A. García-Argáez, L. Dalla Via, D. Passarella, *ACS Med. Chem. Lett.* **2019**, *10*, DOI 10.1021/acsmchemlett.8b00605.
- [32] G. Fumagalli, M. S. Christodoulou, B. Riva, I. Revuelta, C. Marucci, V. Collico, D. Prosperi, S. Riva, D. Perdicchia, I. Bassanini, A. García-Argáez, L. D. Via, D. Passarella, *Org. Biomol. Chem.* **2017**, *15*, 35131.
- [33] I. Bassanini, C. Galli, E. E. Ferrandi, F. Vallone, A. Andolfo, S. Romeo, *Bioconjugate Chem.* **2020**, *31*, 513–519.
- [34] A. Gori, L. Sola, P. Gagni, G. Bruni, M. Liprino, C. Peri, G. Colombo, M. Cretich, M. Chiari, *Bioconjugate Chem.* **2016**, *27*, 2669–2677.
- [35] E. Chiodi, L. Sola, D. Brambilla, M. Cretich, A. M. Marn, M. S. Ünlü, M. Chiari, *Anal. Bioanal. Chem.* **2020**, *412*(14), 1–11.
- [36] W. Trager, J. Jensen, *Science* **1976**, *193*, 673–675.
- [37] S. D'Alessandro, M. Gelati, N. Basilico, E. A. Parati, R. K. Haynes, D. Taramelli, *Toxicology* **2007**, *241*, 66–74.

Manuscript received: July 1, 2022

Revised manuscript received: September 2, 2022

Accepted manuscript online: September 11, 2022

Version of record online: September 26, 2022